International Journal of Mass Spectrometry 305 (2011) iv–ix

Contents lists available at ScienceDirect

International Journal of Mass Spectrometry

journal homepage: www.elsevier.com/locate/ijms

Contents

Editorial

77–77

Editorial

Julie A. Leary

Biobibliography

78–78

Costello biobib

Julie A. Leary

Regular articles

79–86

One-year plasma *N*-linked glycome intra-individual and inter-individual variability in the chicken model of spontaneous ovarian adenocarcinoma

R. Brent Dixon, Michael S. Bereman, James N. Petitte, Adam M. Hawkridge, David C. Muddiman

This study tracks the measured abundance of a number of N-glycans observed from chicken plasma. It provides evidence supporting an individualized approach to diagnostics.

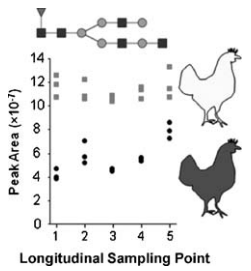

Elsevier B.V.
doi:10.1016/S1387-3806(11)00284-3

87–94

Calmodulin association with the synthetic ERα17p peptide investigated by mass spectrometry

Sandrine Bourgoin-Voillard, Françoise Fournier, Carlos Afonso, Yves Jacquot, Guy Leclercq, Jean-Claude Tabet

The calcium-dependent binding of the PLMIKRSKKNSLALSLT peptide (ERα17p) to *CaM* is probably due to the presence of four basic residues in its sequence.

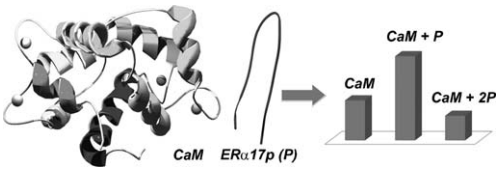

95–102

Top-down high-resolution electron capture dissociation mass spectrometry for comprehensive characterization of post-translational modifications in *Rhesus* monkey cardiac troponin I

Fangmin Xu, Qingge Xu, Xintong Dong, Moltu Guy, Huseyin Guner, Timothy A. Hacker, Ying Ge

► Top-down ECD MS was employed for comprehensively charactering PTMs in monkey cTnI. ► *Rhesus* monkey cTnI was N-terminally acetylated and mono- or bis- phosphorylated. ► Top-down ECD MS unambiguously identified Ser22/Ser23 as the only basally phosphorylated sites. ► The phosphorylation order was determined: Ser23 phosphorylates prior to Ser22. ► No neutral phosphate loss in ECD spectra supports the nonergodic mechanism of ECD.

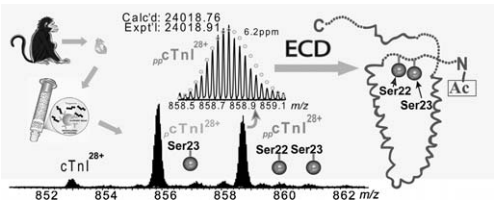

103–108

Analysis of diacylglycerol molecular species in cellular lipid extracts by normal-phase LC-electrospray mass spectrometry

Thomas J. Leiker, Robert M. Barkley, Robert C. Murphy

► Diacylglycerols 2,4-difluorophenyl urethane derivatives. ► Normal phase LC/MS analysis of 1,3- and 1,2-DAG DFPU derivatives ► Monoa-cylglycerols as DFPU derivatives. ► Quantitative analysis in bone marrow derived macrophages. ► Neutral loss scanning of 190 u.

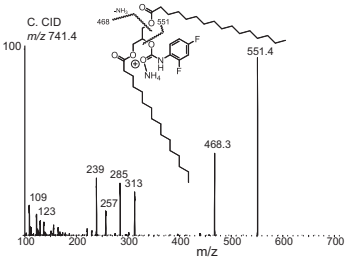

109–115

Electrospray ionization Fourier transform mass spectrometric analysis of intact bikunin glycosaminoglycan from normal human plasma

Tatiana N. Laremore, Franklin E. Leach III, I. Jonathan Amster, Robert J. Linhardt

► Continuous-elution polyacrylamide gel electrophoresis to purify bikunin proteoglycan. ► Electrospray ionization Fourier transform mass spectrometry for intact bikunin glcosaminoglycan chains. ► Plasma bikunin GAG chains consisted predominantly of odd number of saccha-rides.

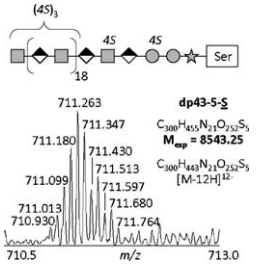

116–119

High mass accuracy and resolution facilitate identification of glycosphingolipids and phospholipids

Huan He, Mark R. Emmett, Carol L. Nilsson, Charles A. Conrad, Alan G. Marshall

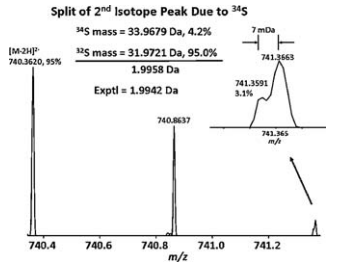

► First resolution of the smallest mass differences in glycosphingolipids (1.6 mDa) andphospholipids (1.8 mDa). ► Ultrahigh mass accuracy FT-ICR MS enables quick assignment of phospholipids and glycosphingolipids from an accurate mass based lipid library. ► Kendrick mass defect analysis is vital for identification and characterization of previously unknown species or species not included in such a library. ► Resolution of isotopic fine structure reveals the presence (and number) of specific atoms in biological glycosphingolipids (e.g., sulfur).

120–130

Fragmentation of negative ions from *N*-linked carbohydrates. Part 5: Anionic *N*-linked glycans

David. J. Harvey, Pauline M. Rudd

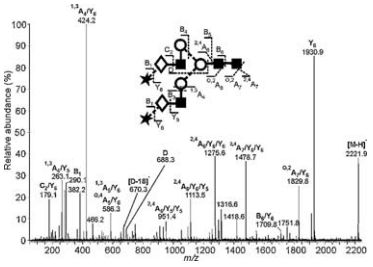

► Negative ion fragmentation of sialylated *N*-linked glycans. ► Ionization is directed mainly by proton loss from acidic groups. ► Diagnostic ions produced by neutral glycans present but usually at lower abundance. ► Sialic acid linkage determined by specific fragments. ► Sialic acids stabilized by Me ester (α2–6-link) or lactone(α2–3-link) formation. ► Spectra of these compounds contain diagnostic ions of enhanced abundance.

131–137

Multistage tandem mass spectrometry of chondroitin sulfate and dermatan sulfate

Alicia M. Bielik, Joseph Zaia

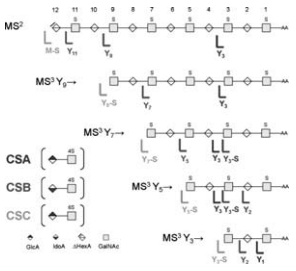

► Multistage tandem MS of chondroitin sulfate. ► Diagnostic product ions for chondroitin sulfate classes. ► Gas phase decomposition of chondroitin sulfate.

138–150

Rapid profiling of bovine and human milk gangliosides by matrix-assisted laser desorption/ionization Fourier transform ion cyclotron resonance mass spectrometry

Hyeyoung Lee, Hyun Joo An, Larry A. Lerno Jr., J. Bruce German, Carlito B. Lebrilla

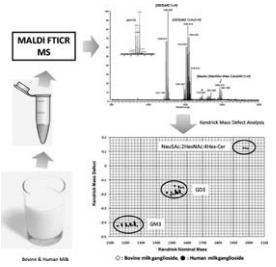

► A rapid and accurate masss pectrometry-based method for profiling gangliosides was demonstrated. ► Ganglioside components have been accurately identified, and in order to accelerate the annotation procedure, Kendrick mass defect analysis has been applied. ► We obtained structural information about the polar headgroup and ceramide backbone by tandem mass spectrometry. ► Bovine and human milk gangliosides differ with respect to the ion intensities of the ganglioside species the distributions of the ceramides. ► These results are necessary for understanding the biological structure–function relationships in complex gangliosides.

151–156

Mass spectrometric analysis of mycothiol levels in wild-type and mycothiol disulfide reductase mutant *Mycobacterium smegmatis*

Cynthia M. Holsclaw, Wilson B. Muse III, Kate S. Carroll, Julie A. Leary

► A novel MS-based method for mycothiol relative quantitation is described. ► Wild-type and *mtr* mutant mycothiol levels were determined. ► The MS-based method is comparable to previously established HPLC-based methods.

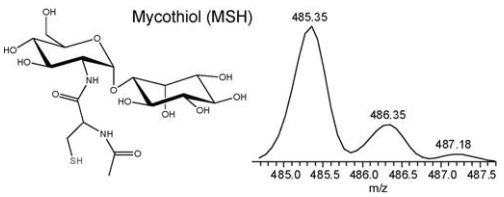

157–163

PEGylated recombinant von Willebrand factor analyzed by means of MALDI-TOF-MS, CGE-on-a-chip and nES-GEMMA

Birgit K. Seyfried, Jürgen Siekmann, Peter L. Turecek, Hans Peter Schwarz, Friedrich Scheiflinger, Harold Zappe, Mary L. Bossard, Günter Allmaier

► Von Willebrand factor (VWF)–largest known human multimeric glycoprotein (up to 20 MegaDa). ► Candidate for therapy of Von Willebrand disease. ► Extrem heterogeneity of PEGylated glycoprotein–recombinant VWF. ► Molecular mass and degree of PEGylation of multiple PEGylated VWF by MALDI-MS and CGE-on-a-chip. ► Size determination PEGylated recombinant VWF by nES-GEMMA.

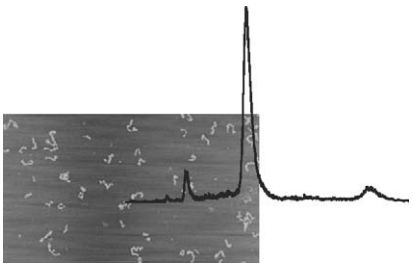

164–169

Infrared matrix-assisted laser desorption/ionization mass spectrometry for quantification of glycosaminoglycans and gangliosides

Michiko Tajiri, Yoshinao Wada

► Generation of multiply deprotonated ions. ► Minimal sulfate group loss from sulfate doligosaccharides. ► No sialic acid loss from polysialylated gangliosides. ► Determination of sulfur content of glycosaminoglycans.

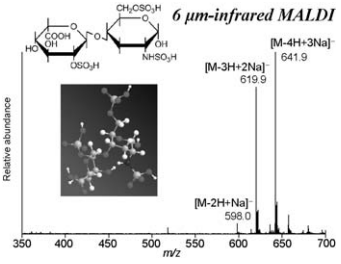

170–177

Electron capture dissociation of divalent metal-adducted sulfated oligosaccharides

Haichuan Liu, Kristina Håkansson

► Sulfated oligosaccharide dications from divalent metal adduction. ► ECD yields extensive fragmentation with sulfate retention. ► CAD mainly results in sulfate loss, precluding sulfate localization.

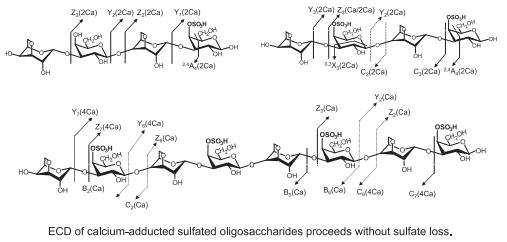

178–184

Concurrent enzyme reactions and binding events for chitinases interacting with chitosan oligosaccharides monitored by high resolution mass spectrometry

F. Henning Cederkvist, Michael Mormann, Martin Froesch, Vincent G.H. Eijsink, Morten Sørlie, Jasna Peter-Katalinić

► Formation of chitooligosaccharide-chitinase non-covalent complexes in the mass range of 55 kDa was dissected by high resolution masss pectrometry. ► Chemical composition of bound and free chitooligosaccharide species and their products in complex mixtures was determined by FT-ICR MS at 9.4T. ► Wild-type chitinase B is shown to undergo with chitooligosaccharides four interaction/reaction pathways: (1) hydrolysis, (2) non-productive binding, (3) transglycosylation, and (4) lactone formation. ► Site-directed mutation D142N in chitinase B is shown to largely enhance the transglycosylation process. ► Site-directed mutagenesis E144Q in chitinase B on the binding specifity to chitooligosaccharides is changed and the enzymatic activity abolished.

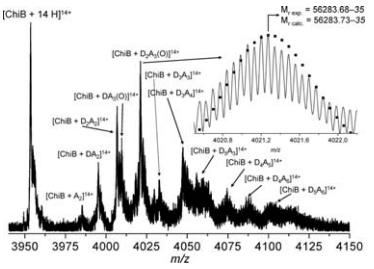

185–198

Glycomic alterations in the highly-abundant and lesser-abundant blood serum protein fractions for patients diagnosed with hepatocellular carcinoma

Pilsoo Kang, Milan Madera, William R. Alley Jr., Radoslav Goldman, Yehia Mechref, Milos V. Novotny

► Glycomic analysis was performed on blood serum glycoproteins subjected to immunoaffinity fraction-ation, resulting in a highly-abundant protein fraction and a lesser abundant protein fraction. ► Several glycans were observed to indicate the presence of liver disease in each fraction. ► The diagnostic glycans indicated different immune and acute-phase responses associated with each disease.

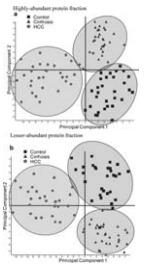

199–208

Fragmentation of neutral oligosaccharides using the MALDI LTQ Orbitrap

Marion Rohmer, Dominic Baeumlisberger, Bernd Stahl, Ute Bahr, Michael Karas

► MALDI LTQ Orbitrap fragmentation of oligosaccharides is possible in both ion modes. ► Complex fucosylated human milk oligosaccharidesare examined. ► Structural analysis of oligosaccharides concerning sequence, linkage and branching. ► The combination of fragmentationtechniques improves sequence coverage.

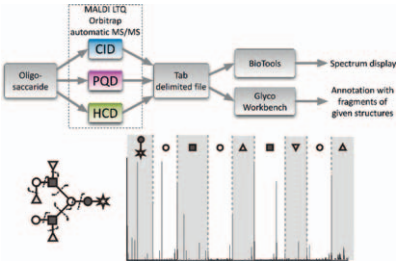

209–216

Methods development for analysis of partially deglycosylated proteins and application to an HIV envelope protein vaccine candidate

Eden P. Go, Geetha S. Hewawasam, Ben J. Ma, Hua-Xin Liao, Barton F. Haynes, Heather Desaire

► A new method for profiling glycosylation site occupancy is introduced. ► The method was applied to a partially deglycosylated Envglycoprotein, which is an HIV vaccine candidate. ► Partial deglycosylation of Env glycoproteins produces a highly heterogeneous product.

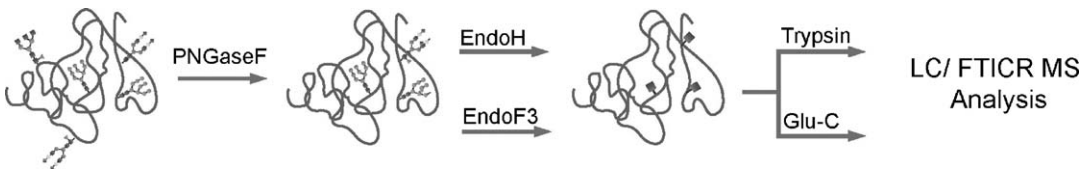

217–227

Degradation and oxidation postmortem of myofibrillar proteins in porcine skeleton muscle revealed by high resolution mass spectrometric proteome analysis

Bogdan Bernevic, Brîndușa Alina Petre, Dmitry Galetskiy, Carsten Werner, Michael Wicke, Karl Schellander, Michael Przybylski

► We report here the identification and structural characterisation of post-mortem degradation and oxidation of myofibrillar proteins using high resolution mass spectrometric proteomics. ► FTICR MS and tandem-MS provided the identification of oxidative modifications. ► The comparison of 2D-oxyblot and silver-stained 2D-gels at low and high drip loss revealed approximately 70 oxidatively modified proteins from muscle cell lysate. ► Oxidative modifications, representing possible biomarker candidates, were identified at Lys-170 of creatine kinase (4-hydroxynonenal), Lys-326 ofactin (amino-adipic semialdehyde), and at W-169 (kynurenine) of triosephosphate isomerase.

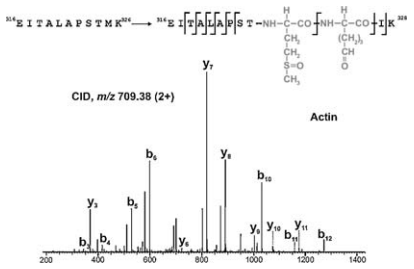

228–237

AP-MALDI imaging of neuropeptides in mouse pituitary gland with 5 μm spatial resolution and high mass accuracy

Sabine Guenther, Andreas Römpp, Wolfgang Kummer, Bernhard Spengler

► MALDI MS and MS/MS imaging of 10 neuropeptides at high spatial resolution(⩽10 μm). ► Reliable neuropeptide identification via accurate mass database search and MS/MS. ► Images gave detailed information on location of individual hormone releasing cells.

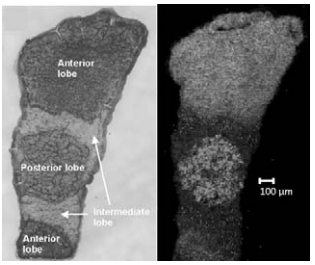

238–246

Characterization of specific binding by mass spectrometry: Associations of *E. coli* citrate synthase with NADH and 2-azidoATP

Vincent C. Chen, Gillian Sadler, Mark E. McComb, Hélène Perreault, Harry W. Duckworth

► Results in this paper help to identify the general allosteric NADH binding pocket of the enzyme citrate synthase. ► Photolabeling experiments using the NADH analogs 2-azido ATP were done to characterize the allosteric site by a combination of mass spectrometry and separation techniques. ► Mass spectrometry results suggest peptide modifications in the area of the pocket previously characterized by X-ray crystallography.